Material Science and Engineering International Research Journal
ISSN: 2997-6685 |
Volume 11 Issue 1, January-March, 2023
Journal Homepage: https://ethanpub.online/Journals/index.php/E29
Official Journal of Ethan Publication

BUCKET LOADING RESISTANCE: INSIGHTS FROM A COMPREHENSIVE DEM STUDY

Wang Wei Jun
School of Intelligent Engineering, Jinzhong College of Information, Jinzhong, 030800, China

Abstract:
The discrete unit method, an approach that conceptualizes a medium as a collection of discrete independent moving units, has found broad utility in building mathematical models based on the properties of these discrete bodies. It treats the subject of analysis as a set of discrete particles, aligning with the inherent characteristics of the discrete bodies themselves. EDEM software, rooted in the discrete unit method, is widely employed across numerous fields for swiftly and efficiently simulating processes. This software empowers in-depth analysis of simulation results, encompassing various aspects like graphical representations, particle tracking, transient analysis, and more. This abstract delves into several notable studies that leverage EDEM software to explore loader shoveling mechanisms. In one study, Yang investigated loader shoveling operations, offering insights into the process and its theoretical foundation [1]. Another researcher, Pang Lizhi, focused on the bucket wheel pick-up process, using EDEM software to simulate the horizontal pick-up process with a power plant's pick-up machine as the subject [2]. Wang introduced a coupling simulation analysis of RecurDyn-EDEM, constructing loader and material models using RecurDyn and EDEM, respectively. The study assessed the coupling effects between the loader's working device and the material under various trajectories [3]. Zheng, addressing real-world material extractor conditions, established an EDEM simulation model for the bucket wheel excavation process. This model, built on the discrete unit method, computed time course curves of excavation resistance for multiple buckets in the material collapse process. These calculations encompassed different burial depths and directions to evaluate maximum excavation resistance hazards under varying conditions [4]. Li, through data processing and simulation parameter setup, devised a shovel loading model within EDEM software for shovel excavation conditions. The model's accuracy was subsequently verified through experimental and simulation methods. The study simulated the shovel loading process and analyzed the resistance experienced by different parts of the bucket at different loading stages to pinpoint the peak of shovel loading resistance [5]. Lastly, Yu examined the characteristics of bulk materials and loader loading conditions, specifically delving into the features of rock materials. This study summarized the calculation methods for determining operating resistance and classified the factors influencing loading resistance during shoveling. The analysis focused on identifying key factors impacting the size of the loading resistance [6].

Keywords: Discrete Unit Method, EDEM Software, Loader Shoveling Mechanisms, Simulation Analysis, Excavation Resistance

1. Introduction

The discrete unit method is to view the medium as a set of discrete independent moving units and to build a mathematical model through the properties of the discrete body, treating the object of analysis as a discrete particle, which corresponds to the properties of the discrete body itself. EDEM software is based on the discrete unit method and is widely used in many fields to calculate simulation processes quickly and efficiently. The software allows detailed analysis of the simulation results, such as graph types, particle tracking, transient analysis, etc. Yang study loader shovelling mechanisms. Includes the shovelling operation process and the theoretical basis[1]. Based on the

Material Science and Engineering International Research Journal
ISSN: 2997-6685 |
Volume 11 Issue 1, January-March, 2023
Journal Homepage: https://ethanpub.online/Journals/index.php/E29
Official Journal of Ethan Publication

discrete element principle, Pang Lizhi studied the bucket wheel pick-up process. Taking the pick-up machine of a power plant as the research object, he applied EDEM software to simulate the horizontal pick-up process[2]. Wang proposed the use of RecurDyn to construct the loader model, and the use of EDEM to construct the material model, and carried out the coupling simulation analysis of RecurDyn-EDEM to study the coupling effect between the loader working device and the material under different trajectories[3]. Zheng according to the collapsed material working conditions occurring in the actual operation of the material extractor, the bucket wheel excavation EDEM simulation model was established by studying the bucket wheel three-dimensional model, combined with the discrete unit method; the time course curves of the excavation resistance of multiple buckets in the material collapse process, under different deep burial conditions and in different directions were calculated, and the calculated values of the bucket wheel excavation resistance in the design specification were compared to assess the hazards of the maximum excavation resistance under different deep burial conditions[4]. Li through data processing and setting of simulation parameters, a shovel loading model was established in EDEM software for shovel excavation conditions, and the accuracy of the model was verified by experimental and simulation methods; afterwards, the shovel loading process was simulated, and the resistance of different parts of the bucket at different stages of shovel loading was analysed to find out where the peak of shovel loading resistance was located[5].The characteristics of the bulk material and the loading conditions of the loader were analyzed by Yu, the characteristics of the rock material were introduced, the calculation methods for calculating the operating resistance were summarized, and the factors influencing the size of the loading resistance were classified in the shovelling process, and the main factors were grasped for analysis [6].

2. Bucket model

The bucket is an important actuator for loading, transporting and discharging materials in the loader's working equipment. It is usually made of the front edge (sometimes equipped with bucket teeth), the bottom of the bucket, the circular bucket wall, the side edge, the side wall and the rear baffle welded together, and the shape in the transverse direction of the body remains basically unchanged, so the geometry of the bucket is determined by the longitudinal section size. At present, the bucket radius of gyration R is usually used as the basic parameter for the calculation of other parameters in the design, with the following formula.

$$R=\sqrt{\frac{V_S}{B_0\left[0.5\lambda_z+\lambda_k\cos\gamma_1\right]-\lambda_r^2\left[\cos\frac{\gamma}{2}-0.5\pi\left(1-\frac{\gamma}{180}\right)\right]}} \quad (1)$$

R: bucket radius of rotation/m; V_s : bucket flat capacity/m^3 ; B_0 : bucket internal measured width/m; λ_g : bucket bottom length coefficient; λ_z : back wall length coefficient; λ_k : baffle height coefficient; λ_r : radius of circle coefficient; γ: opening angle; γ_1 : angle between baffle and back wall

Bulk materials consist of dispersed particles with a bulk substance that is not normally found in solids, liquids and gases, and whose garments of motion follow Newton's second law [7]. Under the action of internal forces, the particles of an object device undergo some kind of flow and take on the characteristics of a liquid, eventually forming a particle flow. In our daily life there are mainly gravel, sand, coal and grains, of which gravel, sand and coal are of most interest. The general rock materials are granite, limestone, sandstone, shale, etc. The characteristic features are different and Table 1 shows the relevant physical properties of crushed rock [8].

Table 1: Physical properties of aggregates

Material Science and Engineering International Research Journal
ISSN: 2997-6685 |
Volume 11 Issue 1, January-March, 2023
Journal Homepage: https://ethanpub.online/Journals/index.php/E29
Official Journal of Ethan Publication

Properties	Numerical values	Properties	Numerical values
Modulus of elasticity E	1.5 x 10^8 N/m^2	Resistance factor	0.20
Density	1.9 x 10^3 kg/m^3	Coefficient ostatic friction	0.90
Friction angle	32.5°	Rolling friction coefficient	0.66
Poisson's ratio	0.35		

3. Non-adhesive spherical particle contact forces (Hertz theory)

The contact model is an important basis for modelling the discrete element method, its description of the contact behaviour between elements and the analytical calculations directly determine the magnitude of the forces and moments applied to the particles. Therefore when using the discrete element method for different objects, the contact models differ and the results vary, but all simulation models must include at least one basic particle-to-particle and particle-to-geometry boundary contact model [9-12]. In this paper, in order to simplify the simulation, the default contact model Hertz theory model set in the EDEM software is used uniformly, which has an efficient and accurate computational performance.

Hertz contact theory assumes that the surfaces of particles in contact with each other are smooth and homogeneous, that the contact surface is small compared to the particle surface, that only elastic deformation occurs at the contact surface, and that the contact force is perpendicular to the contact surface [13-14]. The Hertz contact theory is the theoretical basis of the problem and is applicable to the elastic contact of curved bodies such as spheres, columns and ellipsoids, and even to the contact of micro-convex bodies between contact surfaces. As shown in Fig.1, two spherical particles of radii R_1 and R_2 are in elastic contact, and the normal overlap α is

$$\alpha = R_1 + R_2 - |r_1 - r_2| > 0 \quad (2)$$

The radii of particle 1 and particle 2 are R_1 , R_2; r_1 and r_2 are the spherical position vectors of the two particles respectively.

-62-

The dotted line in Figure 1 shows the location of the particle surface when no deformation is considered, and the contact surface between the particles is circular, then the contact surface radius a is:

$$a = aR^* \quad (3)$$

The inter-particle normal forces N are:

$$N = E^*(R^*)^{\frac{1}{2}}\alpha^{\frac{3}{2}} \quad (4)$$

R* and E* are the effective particle radius and effective modulus of elasticity respectively.

$$\frac{1}{} = \frac{1}{} + \frac{1}{} \quad (5)$$

Material Science and Engineering International Research Journal
ISSN: 2997-6685 |
Volume 11 Issue 1, January-March, 2023
Journal Homepage: https://ethanpub.online/Journals/index.php/E29
Official Journal of Ethan Publication

$$\frac{1}{R^*} = \frac{1-\nu_1^2}{R_1} + \frac{1-\nu_2^2}{R_2} \quad (6)$$

$$\frac{}{E^*} = \frac{}{E_1} + \frac{}{E_2}$$

E_1, ν_1, E_2, ν_2 are the modulus of elasticity and Poisson's ratio of particle 1 and particle 2, respectively.

When the increment of overlap between two contacting particles is $\Delta\alpha$, the increment of normal force ΔN is calculated from (4) or (5).

$$\Delta N = 2\sqrt{\alpha R^* E^* \Delta\alpha} = 2aE^*\Delta\alpha \quad (7)$$

4. Analysis of forward shovelling resistance

4.1 Forces on the bucket in the X, Y and Z directions

The forces on the bucket in the X, Y and Z directions are first analysed. In the simulation, a certain number of gravel particles are loaded into the bucket. The bucket is first shovelled into the rubble pile and then the bucket filled with rubble leaves the pile. The software offers linear translational rotation, sinusoidal translational rotation and convey or translational rotation. Therefore, here we use linear translation and rotation. First, the bucket is shovelled parallel into the pile to a certain depth, then the bucket is turned over and lifted up. Figures 2, 3, 4 and 5 show the variation of forces in the X,Y and Z directions versus time. Where the full shovelling process is 15s. The horizontal axis represents the time of shovelling and the vertical axis represents the amount of shovelling resistance applied in each direction.

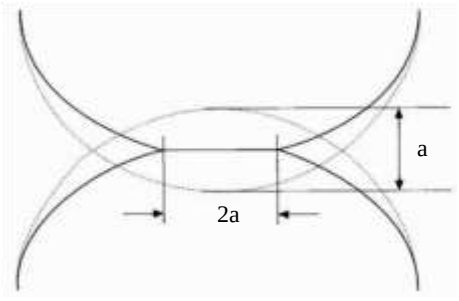

Figure 1: Particle contact deformation diagram

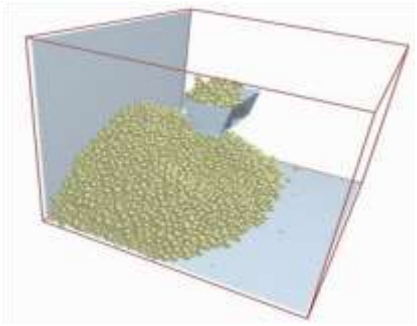

Figure 2: Shovel loading simulation

Analysis of Figure 3 shows that the resistance of the bucket in the X-axis direction exceeds 9KN when the bucket is just shovelling into the rubble pile, there are small fluctuations in the resistance during the process of shovelling into the rubble, but when the bucket is filled with rubble the resistance rises rapidly to 12KN when the bucket is turned over and lifted off the pile, then the maximum partial force falls rapidly to the lowest resistance corresponding to the bucket shovelling out of the rubble pile. The X-directional force then does not change much. The peak force is generated in approximately 1.5s.

Material Science and Engineering International Research Journal
ISSN: 2997-6685 |
Volume 11 Issue 1, January-March, 2023
Journal Homepage: https://ethanpub.online/Journals/index.php/E29
Official Journal of Ethan Publication

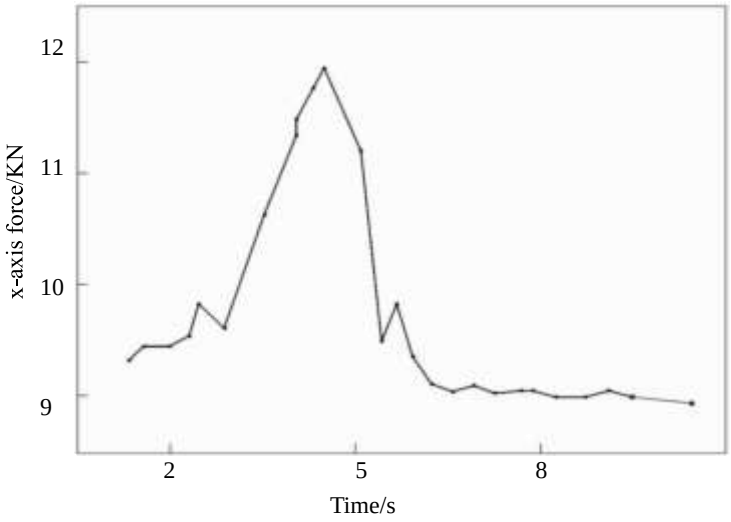

Figure 3: X-directional component of shovel loading resistance

The peak force is approximately 1.5 s. The corresponding force in the Z-axis in Figure 5 is not very large compared to the X and Y-axis. Y-axis is not very large. The rest of the time is very smooth. The z-directional force is much smaller than the x- and y-directions.

Material Science and Engineering International Research Journal
ISSN: 2997-6685 |
Volume 11 Issue 1, January-March, 2023
Journal Homepage: https://ethanpub.online/Journals/index.php/E29
Official Journal of Ethan Publication

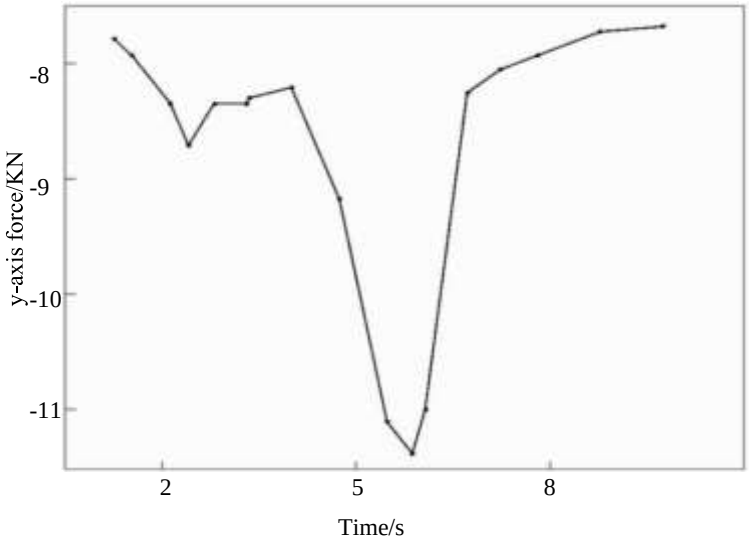

Figure 4: Y-direction of the shovel load resistance

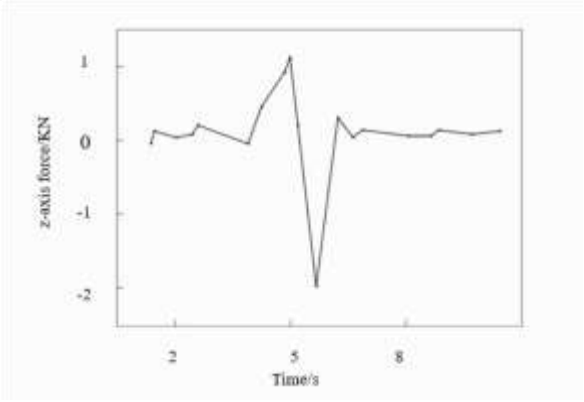

Figure 5: Z-directional component of shovel loading resistance

4.2 Force analysis of the bucket base plate

As the forces exerted on the base plate are the greatest during the shovelling process, the next discussion will focus on the base plate and the left and right plates of the bucket will not be analysed for the time being. Simplifying the actual shovelling process of the loader, the shovel-in phase lasts 7 seconds and the bucket speed is 0.2 m/s; the effective working phase lasts 4 seconds and the angular speed of the bucket is 0.15 arc/s. The forces exerted by the material on the bucket floor during the horizontal shovel-in phase are shown in Figure 6. The forces exerted by the material on the bucket during the bucket reversal lift are shown in Figure 7.

Material Science and Engineering International Research Journal
ISSN: 2997-6685 |
Volume 11 Issue 1, January-March, 2023
Journal Homepage: https://ethanpub.online/Journals/index.php/E29
Official Journal of Ethan Publication

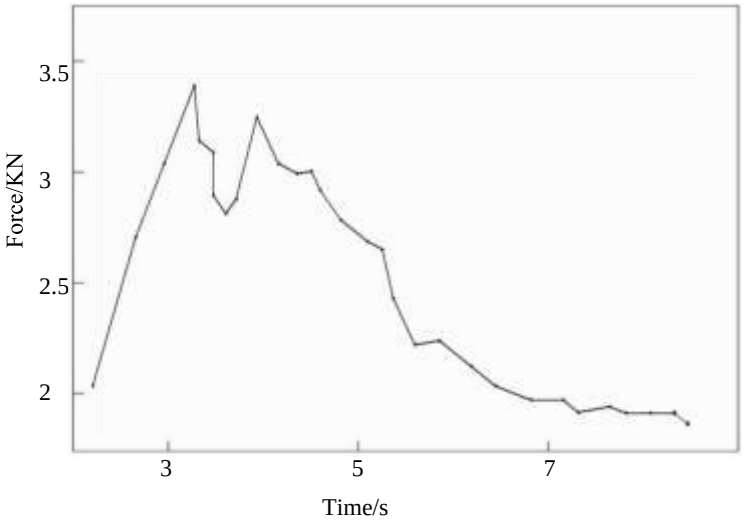

Figure 6: Bucket forces in the horizontal shovel-in phase

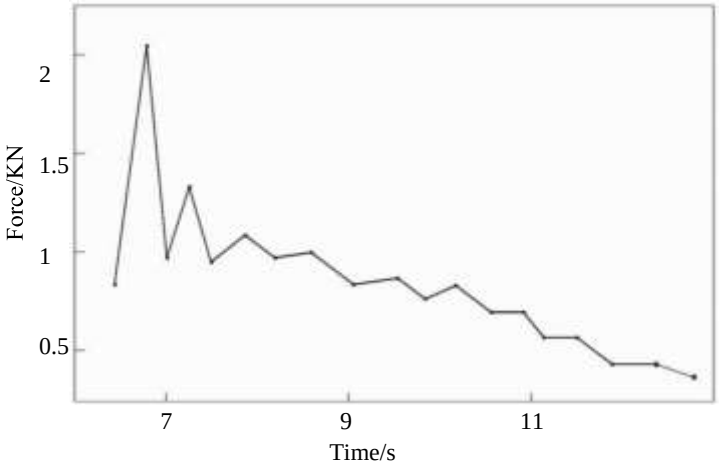

Figure 7: Bucket stress diagram in lifting phase

The analysis of the shovel loading resistance during the horizontal insertion phase showed that during the horizontal insertion phase the total force at the bottom first increased, then decreased and finally stabilised, with local fluctuations during which it showed a secondary peak. The maximum force was 3.5 KN. In the subsequent stages, the force gradually stabilised when the amount of material loaded reached a threshold. As the bucket rotates upwards, the forces previously concentrated at the bottom of the bucket are gradually transferred to the circular wall of the bucket during this phase, so that the forces acting on the bottom of the bucket are significantly reduced during this phase.

5. Results of reverse shovel analysis

5.1 Forces on the bucket in the X, Y and Z directions

Figures 8, 9 and 10 show the relationship between the total force applied to the bucket during excavation in the X, Y and Z directions as a function of time. Where the full shovelling process is 14s. where the horizontal axis indicates the digging time and the vertical axis indicates the magnitude of the digging resistance applied in each direction.

Material Science and Engineering International Research Journal
ISSN: 2997-6685 |
Volume 11 Issue 1, January-March, 2023
Journal Homepage: https://ethanpub.online/Journals/index.php/E29
Official Journal of Ethan Publication

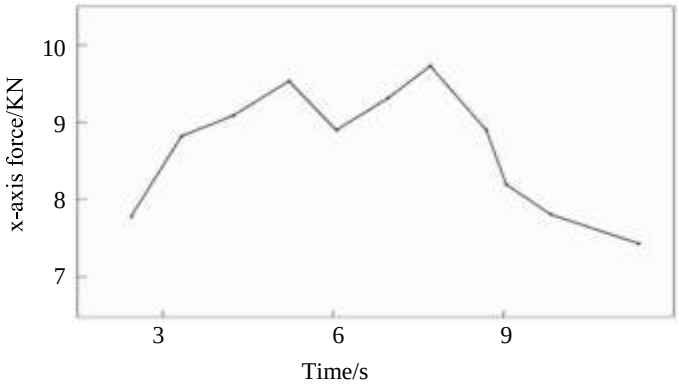

Figure 8: X-directional component of the digging resistance

The relationship between the X-directional force and time can be seen in Figure 8. The resistance of the bucket in the X-direction was just over 7KN when the bucket was just shovelling into the rubble pile, and its X-directional force reached its maximum value of 9.8KN around the 8th s. Between 5.5s and 8s, the bucket force had a more obvious fluctuation. As the time increases, its digging resistance gradually decreases, and after 9s its resistance drops significantly.

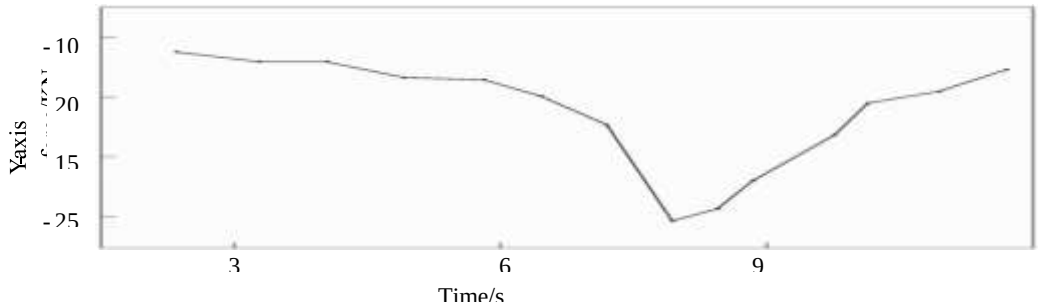

Figure 9: The Y-directional component of the digging resistance

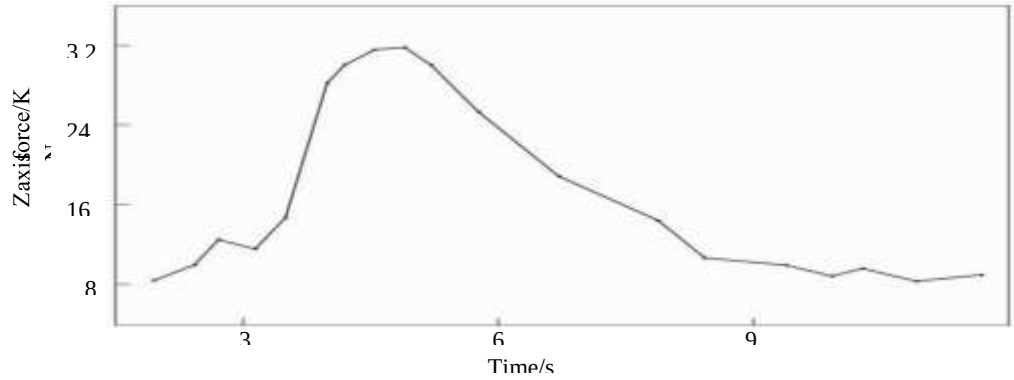

Figure 10: Z-directional component of the digging resistance

From the results of the Y-axis force splitting simulated in Figure 9, it can be seen that the bucket's force splitting decreases gradually from 3 to 7.5s, reaching a minimum of -25KN, and gradually increases after 7.5s. After 6s, the force varies considerably, especially between 7 and 7.5s, when the trend of force decrease is extremely obvious.

Material Science and Engineering International Research Journal
ISSN: 2997-6685 |
Volume 11 Issue 1, January-March, 2023
Journal Homepage: https://ethanpub.online/Journals/index.php/E29
Official Journal of Ethan Publication

The results of the Z-directional forces simulated in Figure 10 show that the bucket's digging resistance gradually tends to increase from 3s onwards, reaching a peak of 32KN at around 5s, and then showing a decline to a minimum of 8KN at the initial resistance.

5.2 Force analysis of the bucket base plate

The following analysis of the horizontal insertion phase of the excavation resistance analysis, in edem derived from the bucket bottom part in the horizontal insertion phase of the force diagram as Figure 11, horizontal insertion phase, the bucket bottom overall force first increase and then decrease, local fluctuations. In the later stages, the forces are gradually stabilised as the amount of excavated material has reached its limit. As the bucket is turned upwards, the bucket floor, which previously bore the main part, is gradually shifted to the circular wall at this stage, so that the forces on the floor at this stage are on a decreasing trend, as shown in Figure 12.

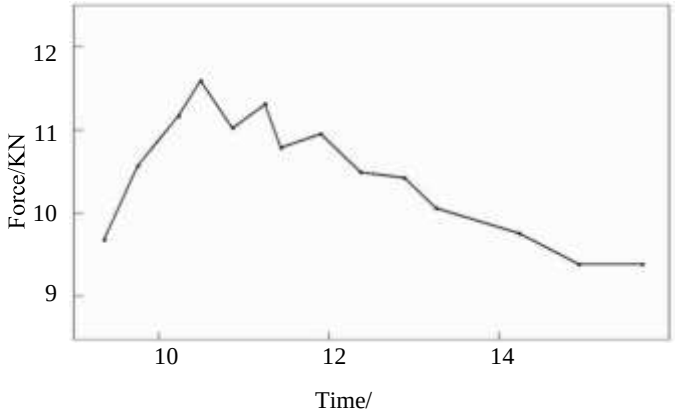

Figure 11: Bucket forces in the horizontal insertion phase

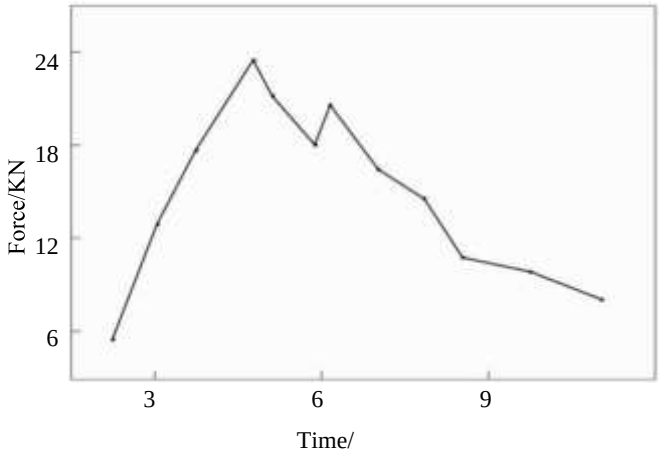

Figure 12: Bucket forces during the pick-up phase

6. Effect of shovel entry angle on resistance

When shovelling horizontally, the bucket is shovelled into the rubble pile at a natural horizontal ground level, but due to the influence of the front teeth of the bucket, the bottom plate of the bucket is tilted at a certain angle to the horizontal surface and cannot achieve true horizontal; while shovelling into the rubble pile at a certain angle, the bottom plate of the bucket must be at a certain angle to the horizontal surface. When the shovel entry angle is less

than 11°, the simulation result is close to the calculated value. In particular, when the shovel entry angle is between 5° and 10°, the two almost coincide. Therefore, we analytically derived the process of shovelling the bucket into the rubble pile, where 7° and 9° were targeted, in order to obtain the best insertion angle. As shown in Figure 13, it is concluded that the shovel entry resistance increases with increasing shovel entry depth, and with increasing shovel entry angle. When the shovel penetration depth is 0.3 m, the effect of the shovel penetration angle on the shovel penetration resistance is relatively small; when the shovel penetration depth exceeds 0.5 m, there is a significant increase in the shovel penetration resistance.

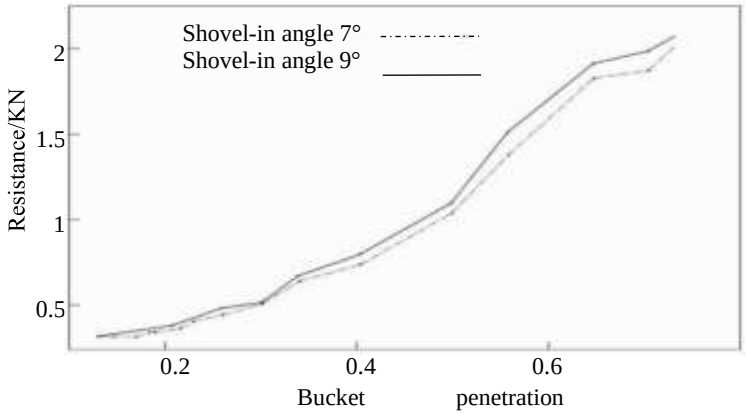

Figure 13: Resistance variation curve

7. Conclusion

Based on the discrete element theory, this paper applies EDEM software to establish a simulation model of the loading process and realise the simulation of the forward and reverse shovelling operation process. Through the simulation, the shovel resistance of different parts of the bucket at different stages of the shovel loading process is analysed, and the parts where the peak shovel resistance is located and the stages where it is located are identified. The resistance of the bucket in the X, Y and Z directions was analysed in the forward and reverse shovelling process. According to the force analysis of the bucket, the force on the bucket floor is the largest, after which the force analysis of the bucket floor during forward and reverse shovelling was carried out to obtain the trend of force changes. Finally, the influence of the shovel entry angle on the resistance was analysed. It can be seen that when the shovel entry angle is 9°, the resistance increases with the depth of shovel entry.

Acknowledgements

This paper was supported by①"2022 Science and Technology Innovation Project for Higher Education Institutions in Shanxi Province (2022L659)"②"2022 Innovation and Entrepreneurship
Project for Students in Shanxi Province(20221640)"

References

Yang Zikang. Research on resistance reduction shoveling strategy of loader based on EDEM [D]. Jilin University, 2022.

Pang, L. C.. Research on the bucket-material interaction mechanism of bucket wheel stacker bucket based on discrete element method [D]. Jilin University, 2022.

Wang Shaojie, Yin Yue, Yu Shengfeng, Hou Liang. Simulation analysis of loader coupling dynamics based on RecurDyn-EDEM [J]. Machine Design,2021,38(11):1-6.

Zheng Pei, Song Wenxi, Hu Xiong. EDEM simulation of excavation resistance of bucket wheel stacker reclaimer under collapsed material condition [J]. Sintered pellets, 2019,44(06):50-54. [5] Li R, Xu Wubin, Li Bing, Yang Xu. Research on discrete unit method for bucket shovel resistance of loader [J]. Journal of Guangxi University of Science and Technology,2017,28(03):77-82.

Yu, Xuebang. Simulation study of loader bucket operation resistance based on EDEM [D]. Guangxi University of Science and Technology, 2018.

Seife C. Can the laws of physics be unified? Science,2005,309(5731): 82-82.

Yan Bo, Zhan Kai, Guo Xin, Li Hengtong, Shi Xiaojie. Simulation study of underground scraper shoveling process based on EDEM [J]. Nonferrous Metals (Mining part),2019, 71(06):74-77. [9] Sun QC, Wang GQ. Introduction to the Mechanics of Particulate Matter. Beijing:Science Press, 2009.

Sun Qicheng, Hou Meiying, Jin Feng. Physics and Mechanics of Particulate Matter. Beijing: Science Press, 2011.

Jaeger HM, Nagel SR, Behringer RP. Granular solids, liquids, and gases. Reu Modern Phgs, 1996, 68(4): 1259-12734.

Kadanoff LP. Built upon sand: theoretical ideas inspiredby granular flows. Rev Modern Phys, 1999, 71(1): 435-4445.

De Gennes PG. Granular matter: a tentative view.RevModern Phys, 1999, 71(2): S374-S382. [14] Forterre Y, Pouliquen O. Flows of dense granular media.Annual Review Flauid Mechanics, 2008, 40: 1-26.